Application of 2D temperature measurement for coal-fired furnace using CT-TDLAS

Zhenzhen Wang[1,2], Wangzheng Zhou[1], Junjie Yan[1,2], Takahiro Kamimoto[2], Kazuma Tsujimoto[2], Yi Li[2], Yoshihiro Deguchi[2,1,*], Nursalwa Ahmad Sani[3], Shazarizul Haziq Samsuri[3], Meor Faisal Zulkifli[3]

[1] State Key Laboratory of Multiphase Flow in Power Engineering, Xi'an Jiaotong University, Xi'an 710049, China
[2] Graduate School of Advanced Technology and Science, Tokushima University, Tokushima 770-8501, Japan
[3] TNB Research Sdn Bhd., Kajang Selangor, 43000, Malaysia

E-mail: ydeguchi@tokushima-u.ac.jp

Received xxxxxx
Accepted for publication xxxxxx
Published xxxxxx

Abstract

The measurement of temperature and species concentrations in combustion fields is very significant to develop the high-efficient combustion technologies for energy conservation and emission reduction. There are various measurement technologies including contact and non-contact measurement. Tunable diode laser absorption spectroscopy (TDLAS) technology is a proven non-contact method to detect the temperature and species concentrations by absorption measurement. To enable two-dimensional (2D) representation of temperature and species concentrations in combustion fields, the TDLAS technology is usually combined with computed tomography (CT). The latter is however considerably new in combustion research, especially in solid fuels reaction environment. In this paper, a 32-path, 2D CT-TDLAS system for temperature measurement in a pilot scale, coal-fired furnace was developed. The accuracy of CT algorithm to reconstruct 2D temperature distributions in different laser-paths arrangements was first analysed using SSD (sum of squared difference) and ZNCC (zero-mean normalized cross-correlation) by comparing to 2D temperature distribution of a full scale coal-fired furnace simulated using computational fluid dynamics (CFD). The accuracy was improved by 32-path reconstruction. The study was then progressed to investigate its accuracy for measurement in a simple CH_4-air burner configuration with rounded and rectangular cells as well as sensitivity for flame shift detection whereby the reconstructed temperature distribution was compared to temperature measured using thermocouple. It is verified that this CT reconstruction was feasible for various measurement areas, even if the center of flame was shifted. Finally, a 32-path, 2D CT-TDLAS system with rectangular structure cell was developed and applied for a temperature measurement in a TNB Research's pilot scale coal-fired furnace. 2D temperature distribution in coal-fired furnace was reconstructed accroding to the experimental results. It is demonstrated the potential of CT-TDLAS for online 2D temperature measurement for actual applications.

Keywords: 2D temperature measurement, 32-path cell, CT-TDLAS, CT reconstruction, Coal-fired furnace

1. Introduction

Combustion phenomena are ubiquitous in different fields, such as power plant, engine, gas turbine, metallurgy and various industrial fields with the energy consumption and pollution emission [1]. Various combustion technologies are developed to improve combustion efficiency and reduce pollution emission, such as fluidized bed combustion, oxy-fuel combustion, optimization of boiler control and so on [2-4]. In coal or gas turbine power plant specifically, combustion temperature and species concentrations are always referred to whenever combustion optimisation effort is taking place. Point temperature measurements (e.g. using thermocouples) and average species detection (e.g. using flue gas analyser) usually install at far downstream locations hinder accurate combustion tuning to be carried-out. To overcome the limitations of these conventional instruments, many efforts have been focusing on new generation sensors development through adopting laser-based technologies. The laser-based temperature or species concentration measurement was found to be of high accuracy. Further, in-situ and online measurement features has made this laser-based sensors superior to its counterpart [5-7]. With the development of laser diagnostics technologies, it has been widely applied to combustion diagnosis in recent decades with the features of accuracy and sensitivity in uniform and non-uniform combustion fields in situ [8-10]. Laser induced fluorescence (LIF) [11], laser-induced breakdown spectroscopy (LIBS) [12,13], coherent anti-Stokes Raman spectroscopy (CARS) [14,15], and tunable diode laser absorption spectroscopy (TDLAS) [16-20], etc. have been applied to different combustion fields for temperature and species concentration measurement.

TDLAS technology has become a proven method of rapid gas diagnostics to detect temperature and species concentrations of molecular components in different combustion areas by absorption measurement [21-23]. In order to accurately acquire the spatial distributions of temperature and concentration in fluid field due to its non-uniform feature, TDLAS technology combined with computed tomography (CT) technology has been developed to measure its two-dimensional (2D) distributions. A hyperspectral tomography (HT) system was designed to simultaneously measure 2D distributions of temperature and H_2O concentration with a temporal resolution of 50 kHz at 225 spatial grid points [24]. A Fourier analysis Abel inversion transform algorithm was utilized to reconstruct 2D distributions of temperature and CO_2 concentration in an axisymmetric flame [25]. A numerical study of multispectral absorption tomography (MAT) with high spatial resolution for combustion flow thermometry was presented for further development and experimental demonstrations [26]. The tomographic method of TDLAS and algebraic reconstruction technique (ART) were studied to detect 2D distributions of temperature, H_2O and NH_3 concentrations in combustion flames and gas flow [27-29]. In order to realize the real-time measurement, an online TDLAS-based tomography system was developed to reconstruct 2D distributions of temperature and H_2O mole fraction with the temporal resolution of 12 ms [30]. The method based on CT and TDLAS named CT-TDLAS was developed for 2D temperature and species concentration measurement using absorption spectra of molecules, such as H_2O, NH_3, CH_4, etc., to demonstrate its applicability for various combustion fields with the high resolution and fast response [31-35]. In our previous studies, 16 laser-paths configuration was mainly utilized to reconstruct 2D temperature and species concentration distributions [31-34].

In this study, a 32-path, 2D CT-TDLAS system with the developed CT reconstruction method for temperature measurement in a pilot scale, coal-fired furnace was developed. 32 laser-paths configurations with rounded and rectangular cells were designed and employed to measure 2D temperature in combustors. The accuracy of CT algorithm to reconstruct 2D temperature distributions in different laser-paths configurations was evaluated and analysed. The measurement accuracy was discussed in a simple CH_4-air burner using 32 laser-paths configuration with rounded and rectangular cells as well as sensitivity for flame shift detection. Finally, the developed 32-path CT-TDLAS system with rectangular structure cell was applied to measure 2D temperature in a TNB Research's pilot scale coal-fired furnace. This CT-TDLAS measurement method will be potential for actual applications of online temperature measurement in combustion fields.

2. Theory

2.1 Computed tomography-tunable diode laser absorption spectroscopy (CT-TDLAS)

Gas temperature and species concentrations can be determined by measuring molecular absorbance at multiple wavelengths using tunable diode laser absorption spectroscopy technique. The principle of TDLAS is based on Beer-Lambert law. When laser beam permeates an absorption medium, the intensity of transmitted light is related to absorber concentration according to Beer-Lambert law. The number density of measured species is related to the amount of absorbed light,

$$I_\lambda / I_{\lambda 0} = \exp\{-A_\lambda\} = \exp\left\{-\sum_i \left[n_i L \sum_j S_{i,j}(T) G_{Vi,j} \right]\right\} \quad (1)$$

Here, $I_{\lambda 0}$ is the incident laser intensity, I_λ is the transmitted laser intensity, A_λ is the absorbance, n_i is the number density of species i, L is the path length, $S_{i,j}$ is the temperature

dependent absorption line strength of absorption line *j*, and $G_{vi,j}$ is the line broadening function. Temperature can be measured by evaluating several absorption lines from same molecule with different temperature dependence [34].

Absorption line strength $S(T)$ can be calculated by following equation,

$$S(T)=S(T_0)\frac{Q(T_0)}{Q(T)}\frac{T_0}{T}\exp\left[-\frac{hcE''}{k}\left(\frac{1}{T}-\frac{1}{T_0}\right)\right]\cdot\frac{1-\exp\left(-\frac{hc\upsilon_0}{kT}\right)}{1-\exp\left(-\frac{hc\upsilon_0}{kT_0}\right)} \tag{2}$$

Here, $Q(T)$ is partition function at particular temperature T and reference temperature T_0=296K, E'' is low transition energy, h is Planck constant, c is light velocity, k is Boltzmann constant, v_0 is laser frequency. According to equation (2), two different absorption lines at same temperature can be used to calculate temperature as follows,

$$S_1(T)=S_1(T_0)\frac{Q(T_0)}{Q(T)}\frac{T_0}{T}\exp\left[-\frac{hcE_1''}{k}\left(\frac{1}{T}-\frac{1}{T_0}\right)\right]\cdot\frac{1-\exp\left(-\frac{hc\upsilon_0}{kT}\right)}{1-\exp\left(-\frac{hc\upsilon_0}{kT_0}\right)} \tag{3}$$

$$S_2(T)=S_2(T_0)\frac{Q(T_0)}{Q(T)}\frac{T_0}{T}\exp\left[-\frac{hcE_2''}{k}\left(\frac{1}{T}-\frac{1}{T_0}\right)\right]\cdot\frac{1-\exp\left(-\frac{hc\upsilon_0}{kT}\right)}{1-\exp\left(-\frac{hc\upsilon_0}{kT_0}\right)} \tag{4}$$

$$T=\frac{\frac{hc}{k}\left(E_2''-E_1''\right)}{\ln\frac{A_1}{A_2}+\ln\frac{S_2(T_0)}{S_1(T_0)}+\frac{hc}{k}\frac{\left(E_2''-E_1''\right)}{T_0}} \tag{5}$$

For 2D measurement, the suitable laser paths will be intersected to each other to form analysis grids for 2D temperature distribution reconstruction by a CT method. When several laser beams are transmitted across the measurement area containing a target gas as shown in Figure 1, integrated absorbance of each laser path is related to the absorber temperature and concentration distribution along the path:

$$A_{\lambda,p}=\sum_q n_{p,q}L_{p,q}\alpha_{\lambda,p,q}=\sum_q n_{p,q}L_{p,q}S_\lambda(T_{p,q})G_{V,\lambda}(n_{p,q},T_{p,q},P) \tag{6}$$

Here, $A_{\lambda,p}$ is integrated absorbance of some wavelength λ in a path, $n_{p,q}$ is the species number density in a path p inside a position q. $\alpha_{\lambda,p,q}$ is absorption coefficient of some wavelength λ at a position q on the path p and is depend on temperature and density of species, $L_{p,q}$ is path length inside the position q. Using a set of equation (6), 2D distributions of concentration and temperature can be reconstructed by CT. In this study, the TDLAS evaluation is based on the spectral fitting method as a function of broadening parameters such as temperature and pressure. The theoretical spectra based on HITRAN database is corrected according to experimental results under various pressure and temperature conditions. A set of measured H_2O absorption spectra is compared to corrected theoretical spectra to minimize the mean squared errors. 2D temperature is determined using a polynomial noise reduction technique. Sets of H_2O densities and temperatures at analysis points are obtained by the best-fitted distributions for a given measurement of $A_{\lambda,p}$ using the minimization procedure shown in Figure 1. The temperature and concentration distributions in the measurement area can be expressed by the following 2D polynomials using the polynomial parameters of a and b, and the polynomial order of m. m is determined by the number of laser paths and the laser path configuration and m is usually chosen as 8-10 for p=16, 10-14 for p=32, and 14-18 for p=64. In this study, p was 32, q was 40, m was 10 and 360 wavelength measurement points were detected during the wavelength scanning. Equation (6) consisted of 11520 equations and there were 132 unknown factors including 66 $a_{k,l}$ and 66 $b_{k,l}$.

$$T(x,y)=\sum_{k=0}^{m}\sum_{l=0}^{k}b_{k-l,l}x^{k-l}y^l \tag{7}$$

$$n(x,y)=\sum_{k=0}^{m}\sum_{l=0}^{k}a_{k-l,l}x^{k-l}y^l \tag{8}$$

In CT-TDLAS calculation, the iterative calculation is performed using the adaptation coefficient replacing the direct use of temperature and concentration as the iteration variable. Temperature and species concentration at each analysis point are determined using a multifunction minimization method to minimize the spectral fitting error.

$$Error=\sum\left[\left(A_{\lambda,p}\right)_{theory}-\left(A_{\lambda,p}\right)_{experiment}\right]^2 \tag{9}$$

When the error is less than a given value, the result is considered to converge. At the same time, the distributions of temperature and concentration in a measurement area can be obtained directly. Therefore, using this CT algorithm, the higher reconstruction accuracy can be obtained. The measurement errors depend on such factors as beam number, view angles, CT-algorism, uncertainty of spectral database, etc. The downhill simplex method for multifunction minimization is used with the merit of its stability for reconstruction especially at the edge of measurement area where the laser path number is usually small compared to that in the center area.

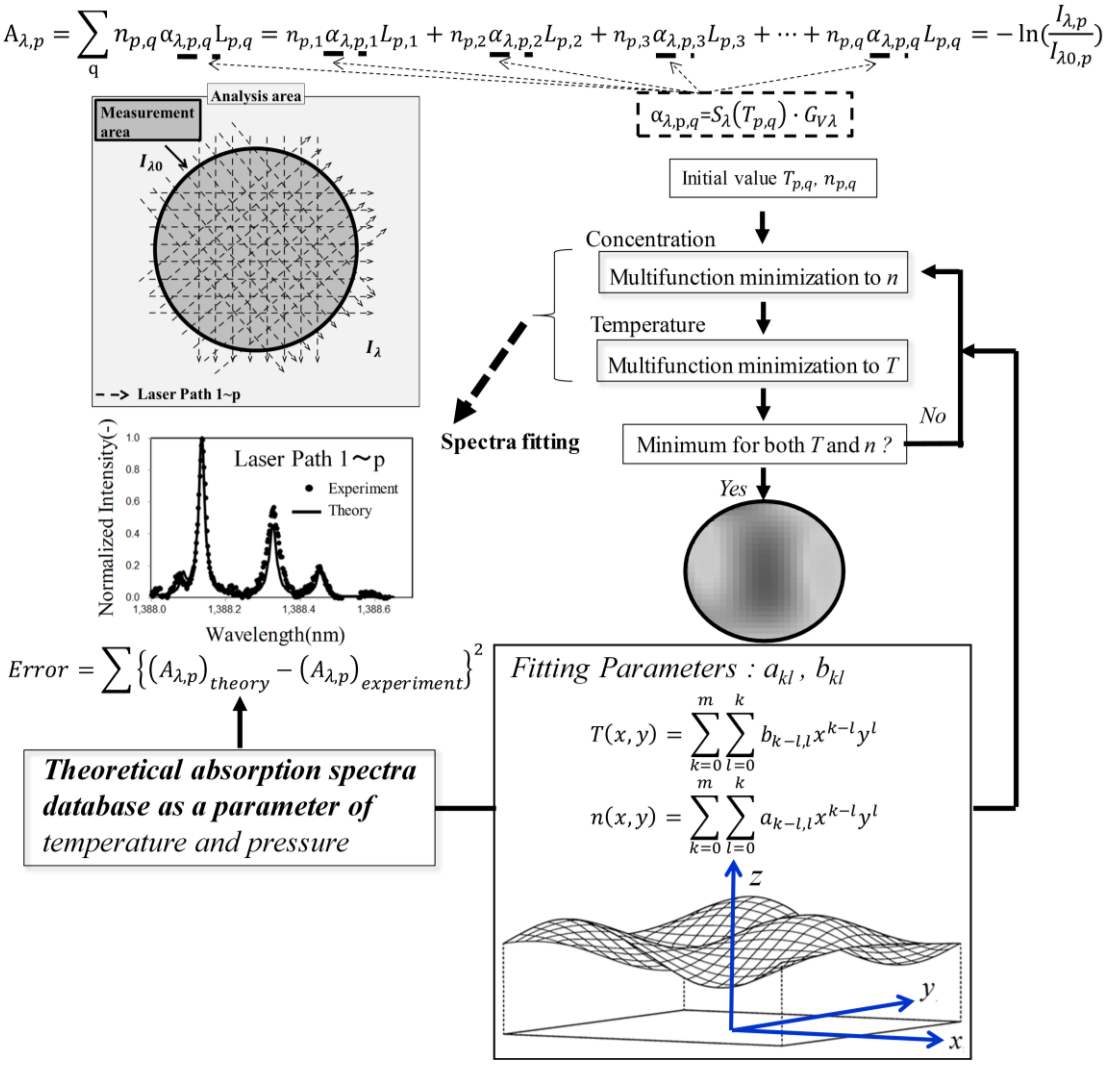

Figure 1 CT-TDLAS algorithm diagram

2.2 Image analysis

The accuracy of CT algorithm was analysed using the approaches described elsewhere [36,37] whereby the sum of squared difference (SSD) and zero-mean normalised cross-correlation (ZNCC) of reconstructed temperature profile were compared to a simulated temperature of a typical full-scale furnace calculated using computer fluid dynamics (CFD). The SSD value is the area range of recognized pattern in the image recognition by comparing the sum of squared difference between the pixels of specified area and the pixels of target pattern, and defined using equation (10), which is divided by the square of the grid number and then divided by the certain temperature to calculate the average relative error of each grid. If the SSD value is closer to "0", the error between CT calculation results and simulation results is smaller with almost same values of two profiles.

The ZNCC value is a zero-mean normalized cross-correlation representing a correlation between CT calculation result and simulation result, and defined using equation (11). If the ZNCC value is closer to "1", the correlation between two profiles is higher with almost same patterns.

$$SSD = \sqrt{\frac{\sum_{x=0}^{X-1}\sum_{y=0}^{Y-1}\left[\left(T_{x,y}\right)_{simulation} - \left(T_{x,y}\right)_{CT-TDLAS}\right]^2}{XY}} / T_R \tag{10}$$

$$ZNCC = \frac{\sum_{x=0}^{X-1}\sum_{y=0}^{Y-1}\left[\left(T_{x,y}-\bar{T}\right)_{simulation}\cdot\left(T_{x,y}-\bar{T}\right)_{CT-TDLAS}\right]}{\sqrt{\sum_{x=0}^{X-1}\sum_{y=0}^{Y-1}\left(T_{x,y}-\bar{T}\right)^2_{simulation}\cdot\sum_{x=0}^{X-1}\sum_{y=0}^{Y-1}\left(T_{x,y}-\bar{T}\right)^2_{CT-TDLAS}}} \tag{11}$$

$$\bar{T} = \frac{\sum_{x=0}^{X-1}\sum_{y=0}^{Y-1}T_{x,y}}{XY}$$

Where, $T_{x,y}$ is the temperature of each point in the measurement area, T_R represents the maximum temperature at 1800K, the subscript simulation represents the CFD

numerical simulation result, and the subscript CT-TDLAS represents the CT calculation result. *X* represents the number of all points in *x* axis of measurement area, and *Y* represents the number of all points in *y* axis of measurement area.

3. Experimental system

The experimental system of temperature measurement and accuracy analysis in Bunsen burner flame using the CT-TDLAS measurement cell is shown in Figure 2. The flow rates of Methane (CH_4) and dried air were 3L/min and 8.5L/min at the pressure of 0.1MPa. The flow rate of air from air compressor was 50L/min to maintain and stabilize the flame. Nitrogen (N_2) as the guard flow was introduced to the measurement cell to purge the laser paths to eliminate the effect of water vapor in ambient gas. The CT measurement cell was installed at a height of 80 mm from the top of Bunsen burner. The 32-path CT-TDLAS measurement cells of rounded structure and rectangular structure were employed in this study. Figure 2(b) and Figure 2(c) illustrate the 32-path configurations of rounded CT cell (Smart Laser & Plasma Systems Co., CT-TDLAS-32LP-HTPC-R60) and rectangular CT cell (Smart Laser & Plasma Systems Co., CT-TDLAS-32LP-LTPC-W93L76Sq). As optical access ports, 32 collimators and 32 detectors were embedded in the 32-path CT-TDLAS measurement cells. Two distributed feedback (DFB) diode lasers (NTT Electronics Co., NLK1E5GAAA/NLK1B5EAAA) near 1388nm and 1343nm were coupled for measurement of absorption spectra in wide temperature range to measure 2D temperature in CH_4-Air flame. Two laser beams were mixed using the 2×2 single mode coupler (Tholabs, 10202A-50-APC) and the mixed laser beam was separated by an optical fiber splitter (OPNETI CO., SMF-28e 1310 nm SWBC 2×16) to 32 paths. The separated laser beams irradiated into the flame by 32 collimators (ETSC, C-1300-2000-KM11). The irradiated laser passed through the access box and the measurement area, and then the transmitted light was detected by 32 photodiodes (Hamamatsu Photonics, G8370-01), amplified by a multi-channel amplifier (Smart Laser & Plasma Systems Co., A-34ch-10db-DC10MHz-IO1M50-SMAJ) and stored in a recorder (Sunki Electric, Memory Hicoder 8861). The temperature of CH_4-Air flame was also measured by a thermocouple (B-type wire diameter 100 μm, Ambie STM), which located at the same measurement height of CT-TDLAS cells, to compare 2D temperature results detected by CT-TDLAS. The temperature measurement using thermocouple was made at intervals of 4mm by moving a micrometer stage.

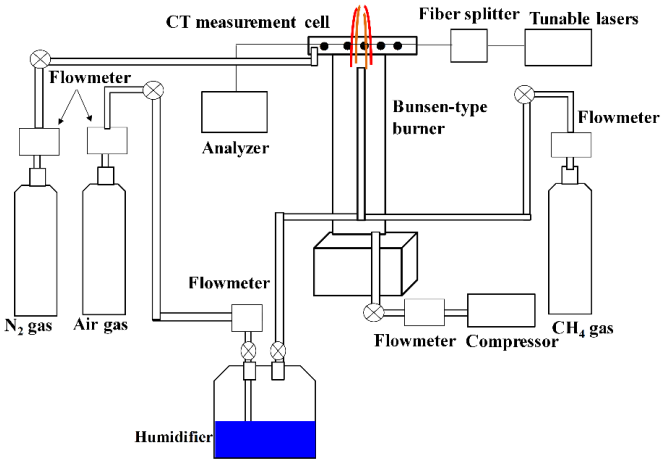

(a) Bunsen burner flame measurement system

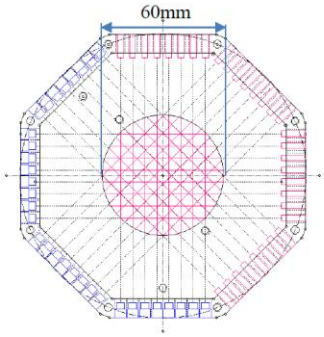

(b) 32-path CT cell of rounded structure

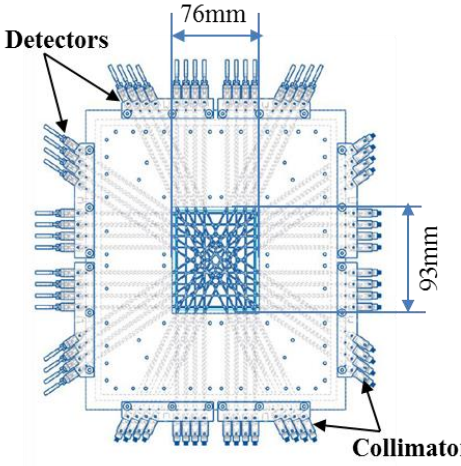

(c) 32-path CT cell of rectangular structure

Figure 2 CT-TDLAS measurement system of Bunsen burner flame

In the second part of this study, the CT-TDLAS technique was assessed in a coal-fired combustion environment. A scaled-down combustor system that mimics actual tangential coal-fired furnaces was designed and fabricated, and is shown in Figure 3. It has an inner working size of 1500 mm (H)◊520 mm (W)◊400 mm (L). To minimise heat loss

through the walls, 100-mm-thick high temperature insulators made from ceramic fiber-board were used. The tangential combustor system consists of a one stage combustion section with two degrees of freedom (x- and y-axis) corner tangential burners. The burners can be adjusted along the x-axis to create and size the imaginary tangential circle diameter (and the fireball in the middle of the combustor) while adjustment along the y-axis (also known as tilting angle) is used to control the flame length. Co-annular burner arrangement was used whereby coal particle (fed using a screw feeder system) was transported using primary air in a steel tube with inner and outer diameter of 15.8 mm and 21.3 mm respectively. The fuel nozzle was centred in an annulus of 54.8 mm inner diameter. There are also four observation layers with four peepholes and thermocouple port at each layer. The interval between one layer to another is 300 mm. Viewing at the lowest level enables flame structure close to the flame base to be monitored while the upper layer ports enable mid-flame and flame tip structure analysis. Bottom and fly ashes can be collected in the bottom collector and cyclone respectively. The combustor is also equipped with a flue gas emission detector, whereby combustion species such CO, SO_2 and NO_x can be monitored and recorded.

For the laser-based temperature sensing system, a 32-path CT-TDLAS system was used which consists of CT cells, DFB lasers, multichannel amplifiers, an AD unit and its related accessories and software. There are four separate CT cell units housing the relevant optic components (two for laser collimation and another two for detection) arranged opposed to each other and secured to the peephole mating flanges as shown in the right image of Figure 3. These cell units can be slotted-in and -out for measurements at different levels. In this current work, the CT-TDLAS cells were installed at the second layer peepholes from the bottom.

Prior to the temperature measurement, the furnace was first heated-up until the temperature at the second layer reaches 1100 K (measured using the thermocouple) using natural gas/ air flame through natural gas swirl burner. This is to ensure the furnace area near the burner contains enough heat for the sample to 'self-ignite'. The coal was then fed into the combustor system and once the temperature stabilised, the natural gas supply was switched-off. A summary of the coal analyses and the operating parameters are shown in Table 1 and Table 2.

Table 1 Coal analyses using analytical fuel test (wt%, as-received)

	Item	Number
Ultimate analysis	Carbon	60.71
	Hydrogen	4.07
	Nitrogen	1.07
	Suphur	0.26
	Oxygen	17.44
Proximate analysis	Moisture	14.83
	Volatile matter	43.03
	Fixed carbon	40.52
	Ash content	1.62

Table 2 Experimental operating parameters

Item	Unit	Number
Coal feed rate	kg/h	10
Primary air flowrate	m^3/hr	12
Secondary air flowrate	m^3/hr	65.3
Excess air	%	10
Particle size	µm	50 - 100

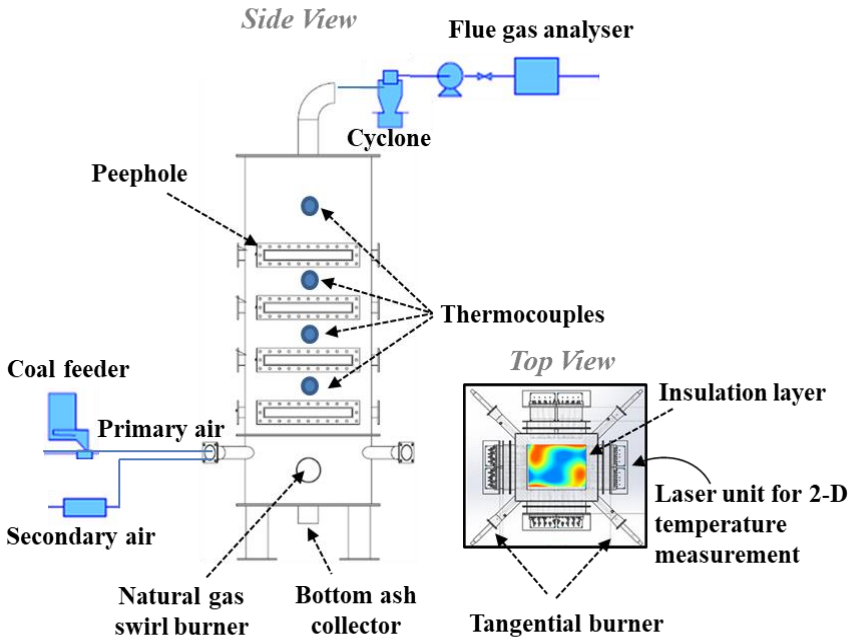

Figure 3 Schematic of 75 kW tangential coal–fired combustor and 2D TDLAS system

4. Results and discussion

One of the merits of TDLAS is high response by continuously scanning laser wavelengths at the rate higher than kHz. The absorbance relating to absorber is used to determine the temperature and concentration, which is not affected by attenuation from dirt or vibration. TDLAS has the ability to eliminate these effects, which is often called "self-calibration". Once a pre-calibration of the TDLAS system is performed, these parameters are not altered by the measurement conditions. The post-calibration necessary for the measurement conditions such as attenuation of laser light intensity can be automatically done at the same rate as the scanning speed of laser wavelength [9]. The 32 laser-paths configuration of rectangular CT-TDLAS cell was designed and applied for a coal-fired furnace. The measurement features of 16 laser-paths CT-TDLAS with rounded cell using rounded cell for Bunsen burner have been studied comprehensively by our group previously [31-34]. In order to evaluate its measurement accuracy of 32 laser-paths configuration using rectangular cell to verify its feasibility, 32 laser-paths configurations of rounded and rectangular structures were designed and applied for Bunsen burner. The rectangular cell for Bunsen burner was the miniature of rectangular CT-TDLAS cell for coal-fired furnace. The temperature measurement accuracy and 32-path CT reconstruction accuracy were evaluated before 2D temperature measurement. H_2O absorption spectra under various temperature and pressure conditions were measured to correct the theoretical spectroscopic database to improve the measurement accuracy. The consistency of theoretical absorption spectra and experimental absorption spectra was increased significantly [31,33]. The different temperature was measured by TDLAS and thermocouple to evaluate the measurement accuracy of TDLAS, which showed the better linearity with the corrected spectroscopic database, as shown in Figure 4(a). The temperature difference between TDLAS with corrected spectroscopic database and thermocouple presented in Figure 4(b) with the maximum difference of 33K in the measurement range of 300K-2000K.

2D temperature distribution can be detected using 32-path CT cells. Each measured spectra can also be detected. Figure 5 shows the measured spectra of Path 1 and Path 5 using 32-path CT cell of rounded structure in Bunsen burner flame. The theoretical absorption spectra with corrected spectroscopic database were consistent with the experimental absorption spectra. In this study, two lasers near 1388nm and 1343nm were mixed to detect H_2O absorptions. Therefore, two different wavelength ranges near 1388nm and 1343nm were detected at the same time from 1 to 300μs due to different laser features of temperature dependence [31]. It is significant to employ several absorption lines with different temperature dependence to reduce the temperature error caused by a CT algorism. Four absorption lines of water vapor located at 1388.135 nm (#1), 1388.326 nm (#2), 1388.454 nm (#3) and 1343.298 nm (#4) with remarkable temperature dependence were compared between experimental and theoretical absorption spectra with corrected spectroscopic database. It was confirmed that the experimental results and the theoretical results presented the consistent spectra. In addition, when comparing path 1 and path 5, it was also confirmed that the distinct absorption spectrum of 1343.298 nm (#4) existed in the high temperature region.

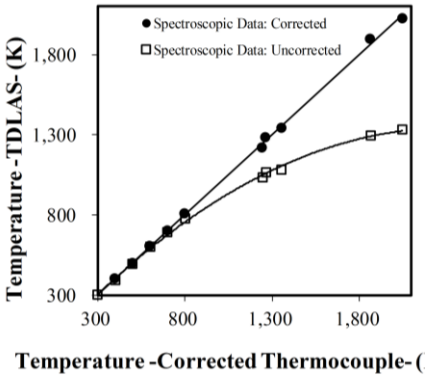

(a) Comparison of TDLAS with/without corrected spectroscopic database and thermocouple

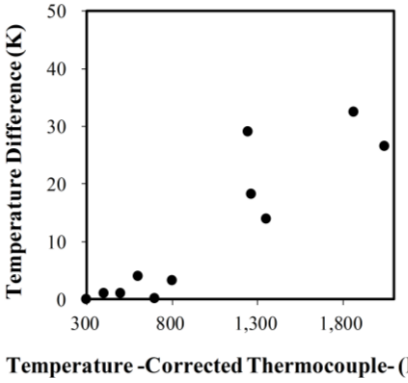

(b) Temperature difference between TDLAS with corrected spectroscopic database and thermocouple

Figure 4 Comparison of measured temperatures by TDLAS and thermocouple

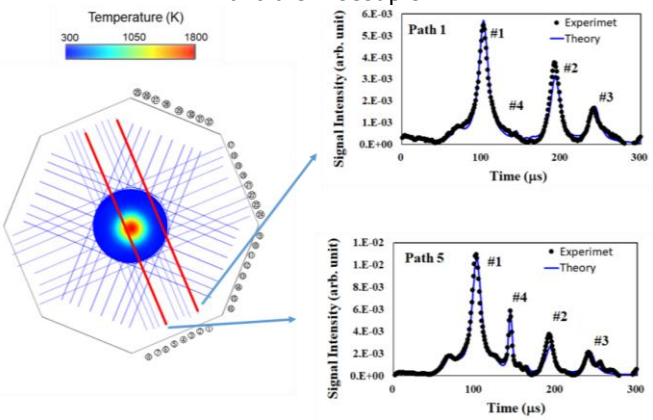

Figure 5 Measured spectra of Path 1 and Path 5 using 32-

path CT cell of rounded structure (1388.135 nm (#1), 1388.326 nm (#2), 1388.454 nm (#3) and 1343.298 nm (#4))

4.1 Evaluation of CT reconstruction accuracy

In this section, the accuracy of CT reconstruction algorithm was evaluated for several reduced laser path test cases, i.e. 16-path, 18-path and two types of 20 paths configurations (red lines) as illustrated in Figure 6, and the result was compared to the standard 32 path case. The analysis was performed using a 2D temperature profile result of a 700MWh sub-critical, tangential coal-fired furnace simulated using ANSYS Fluent. It worth noting that validation of the simulated temperature profile is impossible due to the limitation for 2D temperature measurement in the furnace. A common approach to evaluate the CFD performance, more specifically the overall temperature distribution is through comparing the predicted and actual data of heat absorptions at different heat exchanger zones such as at water wall near the combustion zone, superheater and reheater at upper furnace zone as well as at the furnace rear pass zone as shown in Figure 7. The predicted values are shown to be in a good agreement with the recorded operational data.

The reconstruction results based on the different beam path arrangements are shown in Figure 8. The difference in accuracy between one image to another is hardly observed qualitatively, and hence quantification analysis using SSD and ZNCC approaches described in the previous section was performed.

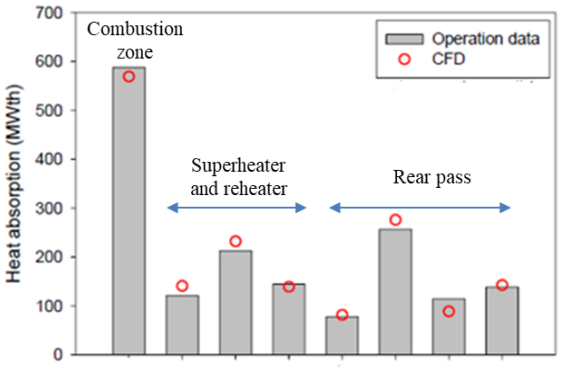

Figure 7 Distribution of heat absorption at different furnace zones

Table 3 lists the accuracy of CT reconstruction using SSD and ZNCC when employing different laser paths. According to the comparison of different laser paths, when increasing the laser paths, the SSD value was closer to "0" and the ZNCC value was closer to "1", which means the accuracy of CT reconstruction increased. Therefore, 32-path CT reconstruction shows the highest accuracy, which can be recognized from Figure 8. However, the laser-paths configuration should also consider the actual measurement area and installation site. In the measurement area of Bunsen burner in this study, some laser paths of 32 paths were tilted in rectangular structure cell as shown in Figure 2(c) compared with that of 32 paths in Figure 6(e) due to the limited measurement area in Bunsen burner. The effect of tilted laser paths was analyzed. The SSD and ZNCC were also 0.055 and 0.91 in both 32 laser-paths, which verified the same CT reconstruction accuracy to obtain the consistent temperature distribution.

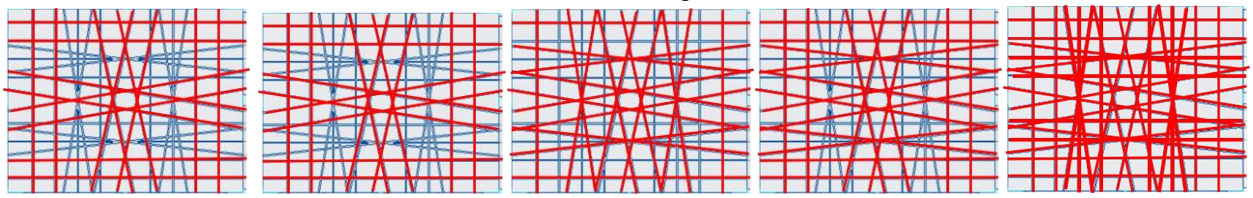

(a) 16 paths (b) 18 paths (c) 20 paths-1 (d) 20 paths-2 (e) 32 paths

Figure 6 16, 18, 20 and 32 laser-paths configurations

Table 3 Accuracy of CT reconstruction

Laser paths	SSD	ZNCC
16 paths	0.068	0.85
18 paths	0.067	0.85
20 paths-1	0.064	0.87
20 paths-2	0.064	0.87
32 paths	0.055	0.91

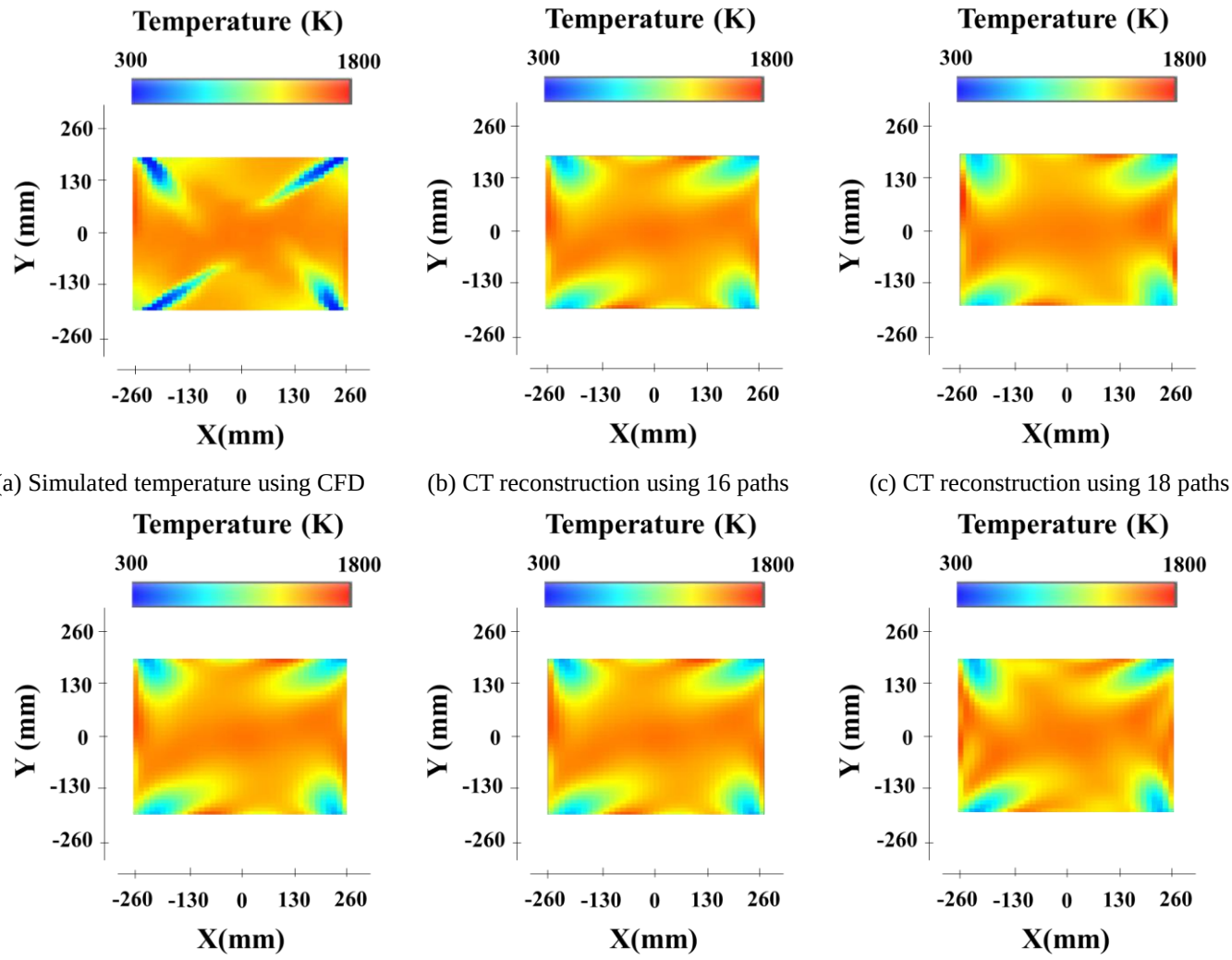

(a) Simulated temperature using CFD (b) CT reconstruction using 16 paths (c) CT reconstruction using 18 paths

(d) CT reconstruction using 20 paths-1 (e) CT reconstruction using 20 paths-2 (f) CT reconstruction using 32 paths

Figure 8 Comparison of temperature distribution between CFD and CT reconstruction results using different laser paths

4.2 Comparison and accuracy analysis of rounded and rectangular cells

According to the evaluation of CT reconstruction accuracy, 32 laser-paths measurement cells of rounded structure and rectangular structure were employed for Bunsen burner to compare and discuss the measurement characteristics of 32-path CT-TDLAS system. 2D temperature distribution was reconstructed by CT algorithm. The temperature distribution was also measured using the thermocouple at the same flame height to form 2D distribution. In the reconstructed area, the pixel of CT-TDLAS was 39 ◊ 39 and the pixel of thermocouple was 12◊12 with the moving step of 4 mm. Figure 9 and Figure 10 illustrate the 2D temperature distributions of rounded 32-path CT cell and rectangular 32-path CT cell measured by CT-TDLAS and thermocouple under the same condition, respectively. The temperature distribution patterns were coincident between CT reconstructed results and thermocouple results. However, the thermocouple results were more divergent. One of the reasons was the minimum spatial scale of features in the reconstructed 2D temperature distribution. It is demonstrated that 2D temperature distribution of CH_4-Air flame can be rapidly and accurately detected and reconstructed using this 32-path CT-TDLAS measurement method in different measurement cells.

In some combustion conditions, the flame is not in the center of measurement area. Therefore, the flame position effect, that is sensitivity for flame shift, was also discussed. When the flame was shifted to one side of the measurement cell, the temperature distribution was measured by CT-TDLAS and thermocouple. Figure 11(a) and Figure 11(b) show 2D temperature distributions of rectangular 32-path CT cell in shifted flame measured by CT-TDLAS and thermocouple, which verified that the CT reconstruction was not influenced by the flame position. In brief, this CT reconstruction is feasible for various laser-paths configurations and measurement conditions.

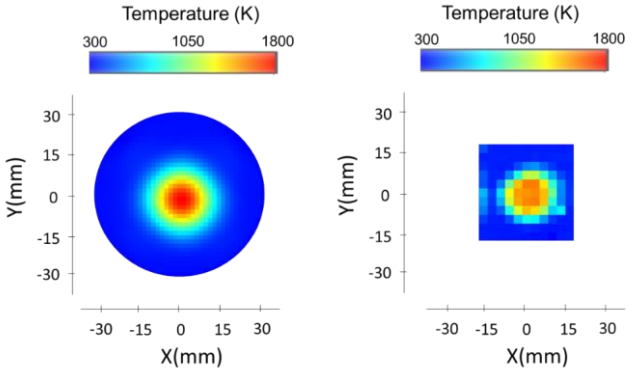

(a) CT-TDLAS results (b) Thermocouple results

Figure 9 2D temperature measurement results of rounded 32-path CT cell

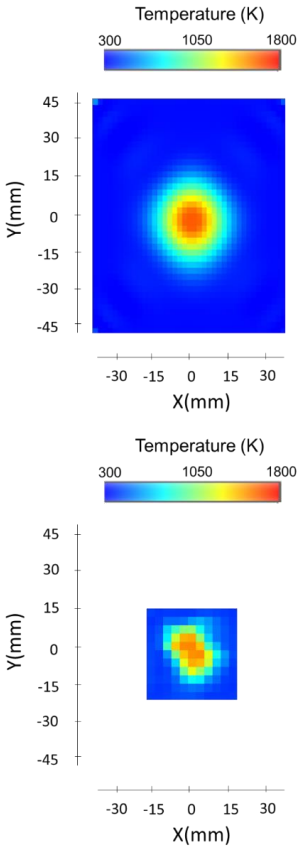

(a) CT-TDLAS results (b) Thermocouple results

Figure 10 2D temperature measurement results of rectangular 32-path CT cell

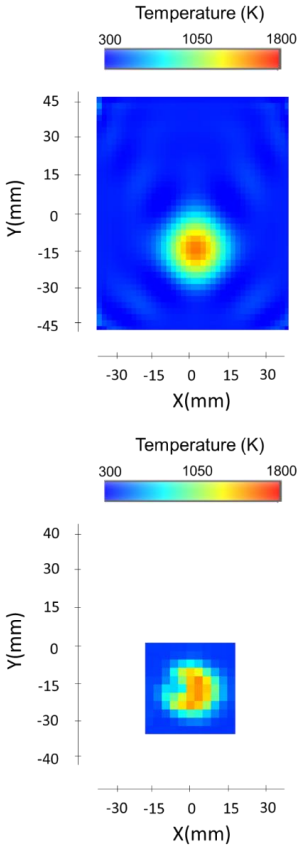

(a) CT-TDLAS results (b) Thermocouple results

Figure 11 2D temperature measurement results of rectangular 32-path CT cell in shifted flame

The quantitative analysis between CT-TDLAS results and thermocouple results were compared in different conditions. The comparisons of path at X=0mm between CT-TDLAS and thermocouple results in rounded 32-path CT cell and rectangular 32-path CT cell are shown in Figures 12(a)-(c). The temperature results measured by the CT-TDLAS method show good agreement with the results measured by the thermocouple. The temperature measured by thermocouple scattered because of the radiation influence. The peak temperature and FWHM (full width at half maxima) in different conditions were also calculated, as listed in Table 4. The measured peak temperature using rounded 32-path CT cell and rectangular 32-path CT cell was almost same when comparing Figure 12(a) and Figure 12(b), as well as the temperature distribution trend at X=0mm. It is confirmed the universality of this CT reconstruction method for different laser-paths configurations. The Bunsen burner flame was controlled by the gas flow rates to maintain the same flame condition for different measurement. However, due to the experimental parameters and surrounding condition effects, the flame could not be identical under all conditions. This is one reason for some difference of temperature distributions, especially for the shifted flame. On the contrary, it is

concluded that the small temperature changes can be detected using this method.

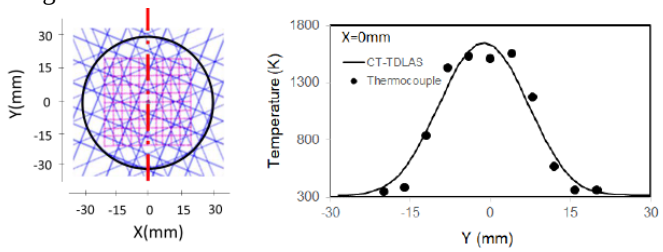

(a) Rounded 32-path CT cell

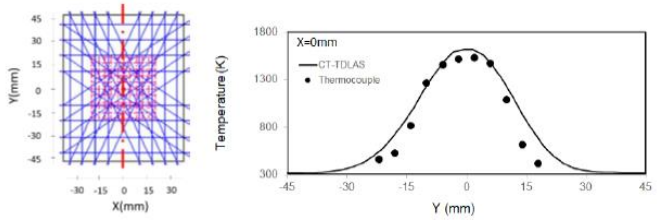

(b) Rectangular 32-path CT cell

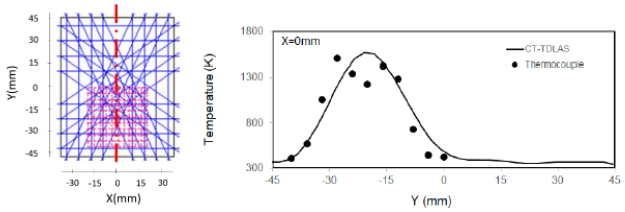

(c) Rectangular 32-path CT cell in shifted flame

Fig.12 Comparison between CT-TDLAS and thermocouple results at X=0mm

Table 4 Comparison between thermocouple and CT-TDLAS

Item	Thermocouple	CT-TDLAS
Peak temperature (rounded cell)	1560K	1650K
FWHM (rounded cell)	26.3mm	26.3mm
Peak temperature (rectangular cell)	1537K	1619K
FWHM (rectangular cell)	30.8mm	30.7mm
Peak temperature (rectangular cell in shifted flame)	1507K	1567K
FWHM (rectangular cell in shifted flame)	29.5mm	31.5mm

4.3 Application of 2D temperature measurement for coal-fired furnace

32 laser-paths CT-TDLAS system was applied for a TNB Research's pilot scale coal-fired furnace to measure its 2D temperature distribution. According to the studies of CT reconstruction and measurement accuracy, as well as its measurement characteristics, the 32 laser-paths rectangular CT-TDLAS measurement cell units was installed in the coal-fired furnace, as shown in Figure 3. In preliminary application condition, the obvious absorption signals of 18 laser paths were detected. One reason for some missed signals was the actual coal-fired flows with a large amount of particles, which accumulated on the windows. The designed flow rate of purged gas was not enough to clean the inner windows of CT-TDLAS cell timely. Therefore, the flow rate of purged gas should be adjusted according to the actual combustion condition and furnace condition to ensure the stable and favorable measurement condition. The measurement results of 18 laser paths were reconstructed using this CT algorithm. Figure 13 shows 2D temperature distribution of coal-fired furnace using CT-TDLAS. The CT reconstruction accuracy of 18 laser paths was presented in Figure 8(c) and Table 3. There were four coal burners at each corner of the furnace. The combustion structure was distinguished on the whole. It is demonstrated the practicability of this CT-TDLAS method. In the actual combustion fields, especially boiler, the 2D temperature distribution inside combustion furnaces is very difficult to be measured by traditional methods, such as thermocouple. Therefore, the proposed CT-TDLAS method in this study is proven to be an effective method for online 2D temperature measurement. The measurement accuracy for real-time applications will be improved by optimizing experimental conditions. The experimental results of 2D temperature distribution can be compared to CFD results to develop the CFD algorithm and adjust the combustion in the future.

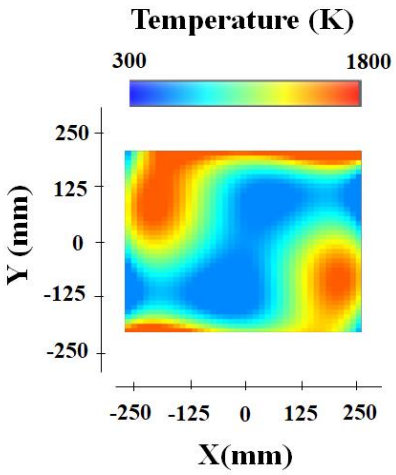

Figure 13 2D temperature distribution in TNB Research's pilot-scale coal-fired furnace

5. Conclusion

32-path CT-TDLAS measurement method was developed and applied in this study to measure 2D temperature distribution of a pilot-scale coal-fired furnace. CT reconstruction accuracy was evaluated according to the temperature distribution of CFD simulation result using SSD and ZNCC in different laser-paths configurations. 32-path configuration presented the highest accuracy in this study. In order to analysis the measurement accuracy and discuss the measurement characteristics of 32-path CT-TDLAS system, the 32-path CT-TDLAS measurement cells with rounded structure and rectangular structure were employed for 2D temperature measurement in Bunsen burner flame as well as sensitivity for flame shift detection whereby the reconstructed temperature distribution was compared to temperature measured using thermocouple. The experimental results demonstrated that this CT reconstruction method is feasible for 2D temperature distribution measurement in different conditions with high accuracy. This 32-path, 2D CT-TDLAS measurement method was successfully applied for the pilot-scale coal-fired furnace to measure 2D temperature distribution. It is demonstrated the potential for online 2D temperature measurement for actual applications.

Acknowledgements

The financial support from Tenaga Nasional Berhad Research (TNB Research) through a research collaboration with Laboratory on Advanced Laser Measurement Technology for Industrial Applications (a joint research laboratory of Xi'an Jiaotong University, China and Tokushima University, Japan) is gratefully acknowledged.

References

[1] BP Statistical Review of World Energy 2019 BP energy outlook.

[2] Scheffknecht G, Al-Makhadmeh L, Schnell U and Maier J 2011 Oxy-fuel coal combustion-A review of the current state-of-the-art *Int. J. Greenhouse Gas Control* **5S** S16-S35

[3] Salinero J, Gómez-Barea A, Fuentes-Cano D and Leckner B 2018 Measurement and theoretical prediction of char temperature oscillation during fluidized bed combustion *Combust. Flame* **192** 190-204

[4] Mortensen J H, Moelbak T, Andersen P and Pedersen T S 1998 Optimization of boiler control to improve the load-following capability of power-plant units *Control Engineering Practice* **6(12)** 1531-1539

[5] Wang D, Song L and Zhang Z 2010 Contact temperature measurement system based on tungsten-rhenium thermocouple *International Conference on Computer Application & System Modeling. IEEE* V12-660-663

[6] Nordine P C, Krishnan S, Weber J K R and Schiffman R A 1991 Non-contact temperature measurement *Adv. Space Res.* **11(7)** 17-31

[7] Ögren Y, Sepman A, Qu Z C, Schmidt F M and Wiinikka H 2017 Comparison of measurement techniques for temperature and soot concentration in premixed, small-scale burner flames *Energy Fuels* **31(10)** 11328-11336

[8] Liu C and Xu L 2018 Laser absorption spectroscopy for combustion diagnosis in reactive flows: A review *Appl. Spectrosc. Rev.* DOI: 10.1080/05704928.2018.1448854

[9] Deguchi Y 2011 Industrial Applications of Laser Diagnostics *CRS Press Taylor & Francis* New York

[10] Deguchi Y, Noda M, Fukuda Y, Ichinose Y, Endo Y, Inada M, Abe Y and Iwasaki S 2002 Industrial applications of temperature and species concentration monitoring using laser diagnostics *Meas. Sci. Technol.* **13** R103-R115

[11] Nygren J, Engstr M J, Walewski J, Kaminski C F and Alden M 2001 Applications and evaluation of two-line atomic LIF thermometry in sooting combustion environments *Meas. Sci. Technol.* **12** 1294-1303

[12] Ctvrtnickova T, Mateo M P, Yanez A and Nicolas G 2011 Application of LIBS and TMA for the determination of combustion predictive indices of coals and coal blends *Appl. Surf. Sci.* **257** 5447-5451

[13] Kiefer J, Trger J W, Li Z, Seeger T, Alden M and Leipertz A 2012 Laser-induced breakdown flame thermometry *Combust. Flame* **159** 3576-3582

[14] Stenhouse I A, Williams D R, Cole J B, and Swords M D 1978 CARS measurements in an internal combustion engine *Appl. Opt.* **18(22)** 3819-3825

[15] Hall R J and Boedeker L R 1984 CARS thermometry in fuel-rich combustion zones *Appl. Opt.* **23(9)** 1340-1346

[16] Wang Y, Wei Y, Liu T, Sun T and Grattan K T V 2018 TDLAS detection of propane/butane gas mixture by using reference gas absorption cells and partial least square (PLS) approach *IEEE Sens. J.* DOI: 10.1109/JSEN.2018.2865508

[17] Zhang Z R, Sun P S, Pang T, Xia H, Cui X J, Li Z, Han L, Wu B, Wang Y, Sigrist M W and Dong F Z 2016 Reconstruction of combustion temperature and gas concentration distributions using line-of-sight tunable diode laser absorption spectroscopy *Opt. Eng.* **55(7)** 076107

[18] Li T, Lin H Y, Zhang H, Svanberg K and Svanberg S 2017 Application of tunable diode laser spectroscopy for the assessment of food quality *Appl. Spectrosc.* **71(5)** 929-938

[19] Cai T D, Gao G Z, Wang M R, Wang G S, Liu Y and Gao X M 2016 High-pressure measurements of temperature and CO_2 concentration using tunable diode lasers at 2 μm *Appl. Spectrosc.* **70(3)** 474-484

[20] Weng W B, Gao Q, Wang Z H, Whiddon R, He Y, Li Z S, Alden M and Cen K F 2017 Quantitative measurement of atomic potassium in plumes over burning solid fuels using infrared-diode laser spectroscopy *Energy Fuels* **31** 2831-2837

[21] Bolshov M A, Kuritsyn Y A, Romanovskii Y V 2015 Tunable diode laser spectroscopy as a technique for combustion diagnostics *Spectrochim. Acta, Part B* **106** 45-66

[22] Hendricks A G, Vandsburger U, Saunders W R and Baumann W T 2006 The use of tunable diode laser absorption spectroscopy for the measurement of flame dynamics *Meas. Sci. Technol.* **17** 139-144

[23] Wang Z Z, Kamimoto T and Deguchi Y 2018 Industrial Applications of Tunable Diode Laser Absorption Spectroscopy Temperature Sensors *InTechOpen* London

[24] Ma L, Li X S, Sanders S T, Caswell A W, Roy S, Plemmons D H and Gord J R 2013 50-kHz-rate 2D imaging of temperature and H_2O concentration at the exhaust plane of a J85 engine using hyperspectral tomography *Opt. Express* **21(1)** 1152-1162

[25] Zhang G Y, Wang G Q, Huang Y, Wang Y Z, Liu X C 2018 Reconstruction and simulation of temperature and CO_2 concentration in an axisymmetric flame based on TDLAS *Optik* **170** 166-177

[26] Cai W W and Kaminski C F 2015 A numerical investigation of high‐resolution multispectral absorption tomography for flow thermometry *Appl. Phys. B* **119** 29-35

[27] Wang F, Cen K F, Li N, Jeffries Jay B, Huang Q X, Yan J H and Chi Y 2010 Two-dimensional tomography for gas concentration and temperature distributions based on tunable diode laser absorption spectroscopy *Meas. Sci. Technol.* **21** 045301(10pp)

[28] Sun P H, Zhang Z R, Li Z, Guo Q and Dong F Z 2017 A study of two dimensional tomography reconstruction of temperature and gas concentration in a combustion field using TDLAS *Appl. Sci.* **7** 990

[29] Wang F, Wu Q, Huang Q X, Zhang H D, Yan J H, Cen K F 2015 Simultaneous measurement of 2-dimensional H_2O concentration and temperature distribution in premixed methane/air flame using TDLAS based tomography technology *Opt. Commun.* **346** 53-63

[30] Xu L J, Liu C, Jing W Y, Cao Z, Xue X and Lin Y Z 2016 Tunable diode laser absorption spectroscopy-based tomography system for on-line monitoring of two-dimensional distributions of temperature and H_2O mole fraction *Rev. Sci. Instrum.* **87** 013101

[31] Kamimoto T, Deguchi Y and Kiyota Y 2015 High temperature field application of two dimensional temperature measurement technology using CT tunable diode laser absorption spectroscopy *Flow Meas. Instrum.* **46** 51-57

[32] Deguchi Y, Kamimoto T and Kiyota Y 2015 Time resolved 2D concentration and temperature measurement using CT tunable laser absorption spectroscopy *Flow Meas. Instrum.* **46** 312-318

[33] Kamimoto T and Deguchi Y 2015 2D Temperature detection characteristics of engine exhaust gases using CT tunable diode laser absorption spectroscopy *Int. J. Mech. Syst. Sci. Eng.* **1** 109

[34] Jeon M G, Deguchi Y, Kamimoto T, Doh D H and Cho G R 2017 Performances of new reconstruction algorithms for CT-TDLAS (computer tomography-tunable diode laser absorption spectroscopy) *Appl. Therm. Eng.* **115** 1148-1160

[35] Hayashi D, Nakai J, Minami M, Fujita K, Kamimoto T and Deguchi Y 2018 CH_4 concentration distribution in a semiconductor process chamber measured by the CT-TDLAS *ECS J. Solid State Sci. Technol.* **7(11)** Q211-Q217

[36] Po L M and Guo K 2007 Transform-domain fast sum of the squared difference computation for H.264/AVC rate-distortion optimization *IEEE Trans. Circuits Syst. Video Technol.* **17(6)** 765-773

[37] Pan B 2011 Recent progress in digital image correlation *Exp. Mech.* **51** 1223-1235